



Published in final edited form as:

Cancer Discov. 2015 September ; 5(9): 960–971. doi:10.1158/2159-8290.CD-15-0063.

Combined EGFR/MEK Inhibition Prevents the Emergence of Resistance in EGFR mutant Lung Cancer

Erin M. Tricker^{#1,2}, Chunxiao Xu^{#1,2}, Sharmeen Uddin^{3,4}, Marzia Capelletti¹, Dalia Ercan¹, Atsuko Ogino¹, Christine A. Pratilas^{3,4}, Neal Rosen^{4,5}, Nathanael S. Gray^{6,7}, Kwok-Kin Wong^{1,2,8,9}, and Pasi A. Jänne^{1,2,8,9,○}

¹Lowe Center for Thoracic Oncology, Dana-Farber Cancer Institute, Boston, MA, 02115, USA.

²Department of Medical Oncology, Dana-Farber Cancer Institute, Boston, MA, 02115, USA.

³Department of Pediatrics, Memorial Sloan Kettering Cancer Center, New York, New York, 10065, USA.

⁴Program in Molecular Pharmacology and Chemistry, Memorial Sloan Kettering Cancer Center, New York, New York, 10065, USA.

⁵Department of Medicine, Memorial Sloane Kettering Cancer Center, New York, New York, 10065, USA

⁶Department of Biological Chemistry and Molecular Pharmacology, Harvard Medical School, Boston, MA, 02115, USA

[○]To whom correspondence should be addressed: Pasi A Jänne, M.D., Ph.D., Dana-Farber Cancer Institute, Lowe Center for Thoracic Oncology, 450 Brookline Avenue, HIM 223, Boston, MA 02215, USA., Phone: (617) 632-6076, Pasi_Janne@dfci.harvard.edu.

P.A. Jänne –

Consultant/Advisory Board

(Minor \$10,000 or less)

Astra Zeneca, Boehringer Ingelheim, Pfizer, Genentech, Clovis Oncology, Merrimack Pharmaceuticals, Chugai, Sanofi

Other

(Major \$10,000 or more)

Lab Corp – post-marketing royalties from DFCI owned intellectual property on EGFR mutations licensed to Lab Corp

Astra Zeneca – sponsored research agreement

(Minor \$10,000 or less)

Inventor on Dana Farber Cancer Institute owned patent on WZ4002 Stock ownership in Gatekeeper Pharmaceuticals

N.S. Gray -

Other

(Minor \$10,000 or less)

Inventor on Dana Farber Cancer Institute owned patent on WZ4002 Stock ownership in Gatekeeper Pharmaceuticals

K.K. Wong

Consultant/Advisory Board

(Minor \$10,000 or less)

AstraZeneca

(Minor \$10,000 or less)

Stock ownership in Gatekeeper Pharmaceuticals

(Major \$10,000 or more)

Astra Zeneca – sponsored research agreement

Chunxiao Xu, Sharmeen Uddin, Marzia Capelletti, Dalia Ercan, Atsuko Ogino, Christine Pratilas, and Neal Rosen-No conflicts of interest

Author contributions: E.M.T., X.C. and P.A.J. designed studies. E.M.T. and M.C. performed laboratory assays and analysis. X.C. and K.K.W. carried out *in vivo* studies. D.E. and A.O. developed cell lines. S.U. and C.A.P. performed quantitative PCR analysis. N.S.G. synthesized Torin2 and WZ4002. E.M.T., C.X. and P.A.J. wrote the paper. All authors reviewed and approved final version of the manuscript.

⁷Department of Cancer Biology, Dana-Farber Cancer Institute, Boston, MA, 02115, USA

⁸Department of Medicine, Brigham and Women's Hospital and Harvard Medical School, Boston, MA, 02115, USA.

⁹Belfer Institute for Applied Cancer Science, Dana-Farber Cancer Institute, Boston, MA, 20115, USA

These authors contributed equally to this work.

Abstract

Irreversible pyrimidine based EGFR inhibitors, including WZ4002, selectively inhibit both EGFR activating and EGFR inhibitor resistant T790M mutations more potently than wild type EGFR. While this class of mutant selective EGFR inhibitors is effective clinically in lung cancer patients harboring *EGFR* T790M, prior preclinical studies demonstrate that acquired resistance can occur through genomic alterations that activate ERK1/2 signaling. Here we find that ERK1/2 reactivation occurs rapidly following WZ4002 treatment. Concomitant inhibition of ERK1/2 by the MEK inhibitor trametinib prevents ERK1/2 reactivation, enhances WZ4002 induced apoptosis and inhibits the emergence of resistance in WZ4002 sensitive models known to acquire resistance via both T790M dependent and independent mechanisms. Resistance to WZ4002 in combination with trametinib eventually emerges due to AKT/mTOR reactivation. These data suggest that initial co-targeting of EGFR and MEK could significantly impede the development of acquired resistance in mutant *EGFR* lung cancer.

Keywords

Lung cancer; EGFR mutation; drug resistance; combination therapy; MEK inhibitor

Introduction

Tyrosine kinase inhibitors (TKIs) such as erlotinib or gefitinib that target the epidermal growth factor receptor (EGFR) are the standard of care for patients with *EGFR* mutant non-small lung cancer (NSCLC) (1, 2). However, TKI therapies are not curative: most patients with *EGFR* mutant NSCLC treated with 1st or 2nd generation EGFR TKIs such as gefitinib, erlotinib and afatinib develop resistance within 9-14 months (1, 2). Extensive research has shown that a variety of mechanisms can lead to acquired drug resistance. The most common mechanism (detected in 60% of patients) is a secondary mutation in *EGFR* itself (*EGFR* T790M) (3-5). Additionally, activation of other kinases (MET, IGF-1R, BRAF, HER2, AXL or FGFRs) or alterations in downstream pathway components (*MAPK1* amplification, PIK3CA activation, *PTEN* loss or *NFI* loss) that bypass the requirement for EGFR to maintain activation of downstream ERK1/2 and AKT pathways can lead to acquired resistance (6-16).

A recent breakthrough in the treatment of *EGFR* T790M mutant cancers occurred with the development of mutant selective pyrimidine based EGFR TKIs, which include the WZ4002, CO-1686, AZD9291 and HM61713 inhibitors (17-19). CO-1686, AZD9291 and HM61713 are in Phase I-III clinical trials and have demonstrated tumor responses in > 50% of patients

with the *EGFR* T790M mutation (20-22). Additionally, their reduced affinity for wild type *EGFR* provokes less toxicity than other TKIs (20-22). However, it is fully anticipated that resistance will also occur to this class of *EGFR* inhibitors. In previous studies, we and others investigated resistance to WZ4002 and found evidence of genetic alterations leading to the *EGFR* independent activation of ERK1/2 (13, 23).

Prior studies have focused on a sequential approach of treatment with *EGFR* TKIs by first identifying mechanisms of resistance to single agent *EGFR* inhibitors and then developing strategies to overcome individual resistance mechanisms. Given the wide variety of identified resistance mechanisms, it is impractical to implement this approach clinically. An alternative strategy is to identify a combination treatment approach that prevents the occurrence of more than one resistance mechanism. This approach could have broad utility as an initial therapeutic treatment or at the time of *EGFR* T790M development. Here we investigate the effectiveness of co-targeting *EGFR* and MEK using *in vitro* and *in vivo* models of *EGFR* inhibitor sensitive and resistant cancers. We demonstrate that this combination is both more effective than single agent WZ4002 at treating cancers with *EGFR* T790M and can also prevent the emergence of both T790M and non-T790M mediated drug resistance. These findings have significant therapeutic implications for patients with *EGFR* mutant NSCLC.

Results

ERK1/2 reactivation occurs after TKI treatment

Preclinical and clinical studies suggest that mutant selective *EGFR* inhibitors are a promising treatment option for T790M positive tumors (17-22). However, it is unclear whether these agents are best used clinically as first line treatment in *EGFR* mutant lung cancer patients or following the development of acquired resistance to current *EGFR* inhibitors. To determine whether resistance is prevented or delayed by initial treatment with mutant selective *EGFR* inhibitors, we assessed the emergence of acquired resistance to gefitinib or to the mutant selective *EGFR* inhibitor tool compound WZ4002 treatment in PC9 cells (which develop T790M in response to gefitinib treatment) (24, 25). Low confluence cells were treated in a 96 well plate format and colonies of 50% confluence were scored weekly (7, 13). We found that both WZ4002 and gefitinib resistant colonies begin to appear within 3-6 weeks, indicating that the emergence of resistance is not delayed by WZ4002 treatment in this cell line (Figure 1A). While ERK1/2 and AKT were initially inhibited to similar degrees, ERK1/2 reactivation was observed within just days following continuous exposure to treatment with gefitinib or WZ4002 (Figure 1B). Next we assessed whether the addition of a MEK inhibitor to WZ4002 was able to maintain ERK inhibition. The MEK inhibitor trametinib effectively inhibits ERK phosphorylation at 30 nM in several *EGFR* mutant cell lines but has little effect on cell viability (Supplemental Figure S1A and S1B). AKT activation is increased by MEK inhibition in some cell lines (e.g. HCC4006, HCC2279) which has been previously reported to be caused by hyperactivation of HER3 (26). TKI naive *EGFR* mutant cell lines (PC9, HCC4006, HCC2279 and HCC2935) treated with WZ4002 + trametinib (W+T) presented with less ERK1/2 reactivation compared to treatment with WZ4002 alone (Figure 1C). Consistent with prolonged inhibition of ERK1/2

phosphorylation, the WZ4002 + trametinib (W+T) combination also significantly sustains inhibition of ERK1/2-dependent gene transcription at 24 hours as compared to WZ4002 alone (Supplemental Figure S1C and S1D) (13, 27).

Prevention versus treatment of acquired resistance

Given that genomic alterations resulting in ERK reactivation also develop following several months of drug exposure and mediate WZ4002 resistance, we sought to determine whether trametinib mediated ERK1/2 inhibition enhances WZ4002 targeted toxicity and prevents the emergence of drug resistance (13). In order to evaluate the effect of W+T on cell viability, we assessed the effect of W+T treatment in TKI naive cell lines (PC9, HCC4006, HCC2279, and HCC2935) at 72 hours (Figure 2A). Overall, the addition of 30 nM trametinib to WZ4002 treatment had a minor impact on cellular viability. While the combination was not synergistic in these short term viability assays, W+T treatment was very effective in preventing the emergence of resistance in TKI naive cell lines; inhibition of growth in response to 100 nM WZ4002 was significantly improved by the addition of 30 nM trametinib as measured by the percentage of colony positive wells at 6 weeks (Figure 2B). It is important to note that these cell lines have diverse yet predictable mechanisms of acquired resistance: PC9 cells are reported to display T790M mutation or IGF-1R activation, HCC4006 cells may develop EMT, HCC827 cells amplify *MET* and HCC2279 cells are resistant to EGFR TKIs due to a reduced ability to induce apoptosis through Bim upregulation (8, 24, 25, 28). Interestingly, the ability of W+T treatment to prevent the emergence of drug resistance was not influenced by these diverse mechanisms.

We next determined whether W+T is effective in delaying the emergence of acquired resistance in cell lines harboring an established T790M mutation, including HCC827 EPR, PC9 GR4, PC9 DR1 and H1975 cells in Figure 2C (for a description of each cell line see Supplemental Table 1). Similar to TKI naive cell lines, the WZ4002 + trametinib combination was able to significantly delay the emergence of acquired resistance and to reduce the incidence of W+T resistant colonies. However, when cell lines harbor established EGFR TKI resistance mechanisms other than the T790M mutation, the combination was less effective (Figure 2D). Combination treatment was able to slightly delay the emergence of resistance but did not affect the overall incidence of acquired resistance in cell lines with pre-existing *MET* amplification (HCC827 GR6 and DFCI81) or activation (HCC827 + HGF) as well as *MAPK1* amplification (PC9 WZR12). Growth of cell lines with EGFR independent activation of the AKT pathway (PC9 Pfr3 and H1650) was not affected by combination treatment. Next, the ability of W+T treatment to reduce the incidence of resistance was assessed at six weeks for all cell lines (Figure 2E). The addition of trametinib to WZ4002 treatment reduced the appearance of colonies in TKI naive and T790M+ cell lines (9 cell lines; 0/9 reached 100% positive wells at 6 weeks and are considered long term “W+T sensitive”), the majority of cell lines with established non-T790M mechanisms of resistance exhibit 100% positive wells at 6 weeks (5/6 cell lines, hereafter defined as “W+T resistant”). Overall, W+T treatment was significantly more effective in TKI naive or T790M + cell but had little effect in most cell lines with non-T790M TKI resistance mechanisms ($p = 0.0020$, Fishers exact test).

As W+T combination treatment prevents the emergence of acquired resistance in EGFR TKI naive cell lines known to develop a variety of TKI resistance mechanisms, we hypothesized that W+T treatment may be superior to combination treatments designed to target just one resistance mechanism predicted to arise in a given cell line. PC9 cells are known to develop *EGFR* T790M or IGF-1R activation as mechanisms of TKI resistance, whereas HCC827 cells develop *MET* amplification (6, 7, 24, 25). To prevent *MET* amplification in HCC827 cells, the clinically used MET inhibitor crizotinib was combined with WZ4002, while PC9 cells were treated with the IGF-1R inhibitor BMS754807 and WZ4002 (Figure 2F). In both cases the targeted combination was able to delay the growth of colonies but not to the extent of W+T treatment. However, WZ4002 + crizotinib was equivalent or superior to W+T when treating HCC827 cells with existing TKI resistance including those with *MET* amplification or aberrant HGF signaling (Supplemental Figure S2).

W+T treatment effectively inhibits S6 activation in sensitive cell lines and enhances apoptosis

To identify predictive biomarkers associated with long term W+T sensitivity, we assessed the ability of W+T treatment to inhibit EGFR dependent signaling cascades, including EGFR, ERK1/2, AKT, and S6 phosphorylation in the HCC827 TKI naive and matching TKI resistant cell lines (Figure 3A). In cell lines that are sensitive to long term W+T treatment (e.g. HCC827 and HCC827 EPR cell lines), EGFR and downstream pathways are inhibited by both WZ4002 and the W+T combination treatment. In cell lines that develop resistance to long term W+T treatment (e.g. HCC827 GR6 and HCC827 + HGF), EGFR and ERK1/2 are efficiently inhibited by W+T combination treatment but AKT and S6 inhibition were impaired. EGFR, ERK1/2, AKT and S6 phosphorylation were then assessed in the complete panel of cell lines shown in Figure 2E (Supplemental Figure S3). In the majority of W+T sensitive cell lines, WZ4002 alone or W+T treatment reduced the activity of EGFR dependent pathways. W+T resistant cell lines treated with W+T exhibited reduced EGFR and ERK1/2 activation but S6 activation was unchanged. An exception was seen with the H1975 cell line, wherein WZ4002 or W+T treatment did not inhibit S6 activation despite a W+T mediated reduction in the emergence of drug resistance at six weeks (as shown in Figure 2C). However, this cell line generates a high frequency of W+T resistant clones compared to other TKI naive or T790M+ cell lines and is possibly an example of a cell line with moderate sensitivity to long term W+T treatment.

Next we sought to define the mechanism of W+T activity. Both EGFR and MEK inhibitors can induce apoptosis, in part through the upregulation of Bim (29-31). We assessed Bim levels in each cell line after a 24 hour treatment with WZ4002, trametinib or a combination thereof (Figure 3B). Both W+T sensitive and resistant cell lines induced Bim in response to WZ4002 or trametinib treatment, but there was no correlation between the level of Bim upregulation and prevention of acquired resistance. While Bim has been reported as necessary to induce apoptosis in response to EGFR TKIs and to MEK inhibitors, it is not always sufficient to induce apoptosis (32). Therefore we assessed caspase 3 activity levels after WZ4002, trametinib or combination treatment (Figure 3C). Increased caspase 3 activity was more frequent in W+T sensitive cell lines (6/9) compared to W+T resistant cell lines (2/6), and the magnitude of increased caspase 3 activity levels was greater in sensitive cell

lines; in 8/9 sensitive cell lines the fold change in caspase 3 activity was greater than 2.5 fold, whereas 1/6 cell lines resistant to long term W+T treatment exhibited a similar increase ($p = 0.0110$, Fishers exact test).

EGFR/MEK inhibition improves in vivo response

To determine whether the *in vitro* superiority of the W+T combination over WZ4002 is recapitulated *in vivo*, mice harboring xenografts of PC9 GR4 cells (*EGFR* DelE746_A750/T790M) were treated with WZ4002, trametinib or the combination thereof. During the course of treatment both WZ4002 alone or in combination with trametinib led to significant tumor regressions (Figure 4A). Biochemical assessment of tumor lysates indicated that W+T treatment improved ERK1/2 inhibition over WZ4002 alone after two and four doses (Supplemental Figure S4A and SB). As both WZ4002 alone and W+T treatment reduced tumor burden to undetectable levels, we assessed tumor growth following treatment cessation to determine if these tumors were completely eliminated (termed here “tumor cure”). After treatment cessation all tumors treated with WZ4002 alone began to rebound, whereas in W+T treated mice outgrowth was observed in only 7/15 subjects. In cases where tumor outgrowth in W+T treated mice was detected, the tumors were significantly smaller than those treated with WZ4002 alone (Supplemental Figure S4C). Similar results were seen in the gefitinib sensitive PC9 (*EGFR* DelE746_A750) xenografts, albeit single agent treatments were more effective than in the PC9 GR4 xenograft model, with 4/15 tumor cures after WZ4002 treatment, 1/15 tumor cures after trametinib treatment and 7/15 tumor cures after combination treatment (Figure 4B). Xenograft models using the H1975 (*EGFR* L858R/T790M) cell line (which generate a higher percentage of resistant clones *in vitro* than the PC9 and PC9 GR4 cell lines, Figure 2C) were also examined after treatment with single agents and the W+T combination and while the combination was able to prevent tumor outgrowth for at least 14 weeks, no tumor cures were observed after treatment cessation (Figure 4C).

We further evaluated the efficacy of the W+T combination in a genetically engineered mouse model (GEMM) of *EGFR* L858R/T790M (LT) NSCLC. This model was previously demonstrated to exhibit ERK1/2 reactivation after generation of WZ4002 resistance (13). Initially, tumor regression occurs in both WZ4002 and W+T treatment groups but the combination is significantly more effective (Figure 5A, at two weeks, $p = 0.0041$, two tailed t test). Immunohistochemical (IHC) analysis following two doses of treatment demonstrates that inhibition of EGFR, ERK and AKT are similar between WZ4002 and W+T, (Figure 5B, Supplemental Figure S5A). A significant increase in apoptosis was observed in tumors from mice treated with W+T compared to individual treatments as analyzed by terminal deoxynucleotidyl transferase dUTP nick end labeling (TUNEL) staining (Figure 5C and D, Supplemental Figure S5B). Treatment differences between WZ4002 and W+T conditions become more apparent after two weeks; tumors treated with WZ4002 or trametinib began to rebound while W+T treated tumors were inhibited beyond 20 weeks (Figure 5E and Supplemental Figure S5C and D). Trametinib alone was unable to prevent tumor growth, and the addition of WZ4002 to trametinib at the time of tumor regrowth caused a transient reduction in tumor volume. Overall, W+T treatment was able to significantly extend the survival of mice beyond WZ4002 alone (Figure 5F, $p = 0.0097$; log-rank test).

Mechanisms of acquired resistance to EGFR/MEK inhibition

To study W+T acquired resistance, we continued W+T treatment of the LT GEMMs until tumor outgrowth was observed (Supplemental Figure S6A and S6B). These tumors were harvested and the EGFR signaling pathway was assessed by IHC to identify any reactivated components. Phosphorylation of EGFR and ERK1/2 was assessed and S6 and 4EBP1 were also evaluated as a readout of the mTOR pathway (Figure 6A and Supplemental Figure S6C). Notably, we found an unusual degree of heterogeneity between adjacent tumor nodules in each mouse, and were able to identify tumor nodules with significant phosphorylation residing next to nodules in which phosphorylation was not detected for EGFR, ERK1/2, S6 and 4EBP1 (Figure 6A). However, EGFR and ERK1/2 inhibition by the W+T combination was maintained in the majority of resistant nodules whereas S6 was frequently re-activated, occurring in 18/27 (67%) tumor nodules examined (Figure 6B). Reactivation of both AKT and S6 was also detected by western blot of tumor lysates (Supplemental Figure S6D). However, no genetic lesions known to increase mTOR activation (e.g. PTEN, AKT1, TSC1, TSC2, p85 α , PI3KCA) were identified in these resistant tumors (data not shown). To confirm the impact of mTOR signaling on W+T resistant tumors, we administered the TORC1/2 inhibitor Torin2 with the W+T combination in two mice exhibiting W+T resistance and assessed changes in tumor volume for four weeks (Figure 6C) (33). Torin2 has minimal activity by itself (data not shown). In both cases, the addition of Torin2 to W+T treatment resulted in tumor shrinkage (Figure 6D).

To determine if mTOR activation is also observed after W+T resistance is generated *in vitro*, PC9 cells were seeded in 96 well plates at low confluence and treated weekly with W+T until resistant clones emerged. These drug tolerant populations were then treated with W+T for eight hours and EGFR, AKT, ERK1/2 and S6 inhibition were assessed (Figure 6E). While W+T could still inhibit EGFR and ERK1/2 phosphorylation, AKT and S6 phosphorylation were unaffected by treatment. Torin2 treatment alone was able to inhibit S6 phosphorylation and decrease the viability of both the parental and W+T drug tolerant populations (Supplemental Figure S7A and B). Furthermore, the addition of Torin2 to W+T combination treatment was able to restore sensitivity of the PC9 W+T resistant cells almost to that of the parental PC9 levels (Figure 6F, Supplemental Figure S7C).

Discussion

The development of acquired drug resistance limits the long-term clinical success of EGFR inhibitors in lung cancer. The identification and clinical development of mutant selective EGFR inhibitors provides the opportunity to both treat patients with *EGFR* T790M mediated drug resistance and to develop combination treatment approaches that previously were not possible due to combined toxicity of EGFR inhibitors and agents targeting signal transduction pathways.

Here we propose that co-targeting EGFR and MEK is a more effective combination strategy than just targeting EGFR alone. There are two potential uses for this approach. The addition of a MEK inhibitor can enhance the efficacy of WZ4002 in *EGFR* T790M containing models. Through the use of *in vitro* models, xenograft models and *EGFR* L858R/T790M GEMMs, we demonstrate that the W+T combination is significantly better at delaying the

onset of resistance than WZ4002 alone, and cures some xenograft models (Figures 2, 4 and 5). A second clinical use for this combination is the prevention of drug resistance, which has broad clinical applicability as our studies demonstrate that the W+T combination prevents both T790M dependent and independent drug resistance (Figure 2). Compared to WZ4002 alone, this combination was able to cure a fraction of tumors in the xenograft models. While this represents an improvement over the single agent, these data suggest that additional strategies are still needed and provide a starting point for the development of effective combination strategies using EGFR TKIs. In fact, this approach is better than a preventative treatment designed for the specific resistance mechanism known to arise as a result of EGFR inhibition (e.g. MET/EGFR inhibition in HCC827 cells that develop *MET* amplification in response to EGFR inhibitors).

In contrast, the W+T combination is relatively ineffective in models with established non-T790M acquired resistance, likely because compensatory pathways allows for proliferation even in the presence of combined EGFR/MEK inhibition (Figure 2D). Our studies suggest that one such pathway is the mTOR pathway as W+T is unable to downregulate S6 phosphorylation in the majority of resistant cell lines, in contrast to sensitive cell lines (Figure 3A). Additionally, acquired resistance to W+T treatment in LT GEMMs and PC9 cells is associated with S6 reactivation (Figure 6). Further support for the significance of the mTOR pathway in resistance to W+T treatment is seen by the ability of the mTOR inhibitor Torin2 to re-sensitize cells to W+T treatment both *in vitro* and *in vivo* (Figure 6). The mTOR pathway is a convergence point for many signaling pathways including EGFR and other receptor tyrosine kinases, and additionally can be affected by mutation or loss of tumor suppressors such as PTEN, TSC1 or NF2 (34). As mTOR and downstream S6 activation can occur in response to a diverse array of survival signals, S6 may have utility as a general biomarker for optimal TKI response. S6 has also been reported as a putative biomarker for response to RAF or MEK inhibitors in melanoma and for afatinib + cetuximab combination treatment in NSCLC (35, 36).

The enhanced efficacy of the W+T combination compared to WZ4002 alone is likely due to at least two mechanisms. The addition of a MEK inhibitor provides more prolonged and effective pathway inhibition than WZ4002 alone (Figures 1C) and hence may lead to a delay in the onset of resistance. Genetic alterations leading to ERK reactivation have also been identified in preclinical models of single agent EGFR TKI resistance (13). Additionally, reactivation of ERK1/2 signaling has also been observed in preclinical models of drug resistance to AZD9291 suggesting that this observation is not WZ4002 specific (23). A second mechanism contributing to the enhanced efficacy of W+T that may be a result of enhanced pathway inhibition is the increase in apoptosis observed both *in vitro* (Figure 3C) and *in vivo* (Figure 5C and 5D). It is possible that in the presence of this increased apoptotic effect it is more difficult for a resistant clone to emerge, especially when cell proliferation may be compromised because of MEK inhibition. In accordance with this hypothesis, many of the observations demonstrating the enhanced efficacy of the W+T combination are only evident in long term *in vitro* and *in vivo* studies. The relative contributions of these two mechanisms, more effective pathway inhibition and enhanced apoptosis, to the improved *in vitro* and *in vivo* efficacy observed with the WZ4002 and trametinib combination remains to be determined.

The success of WZ4002+trametinib in preventing and treating drug resistance suggests that this combination may be of use clinically and more effective than single agent therapy with mutant selective inhibitors such as AZD9291 or CO-1686. Our study provides guidance as to where this combination should be evaluated, specifically either as initial therapy in EGFR TKI naïve patients or in those that have developed *EGFR* T790M mediated drug resistance. However, clinical trials will be required to confirm superior efficacy and tolerability in lung cancer patients. An ongoing clinical trial is evaluating the combination of AZD9291 and the MEK inhibitor selumetinib (NCT02143466) and findings from this study will further inform the best strategy to prevent or treat drug resistance in *EGFR* mutant lung cancer patients. These studies will provide a starting point towards improving EGFR TKI combination strategies.

Materials and Methods

Cell lines and reagents

NSCLC cell lines PC9, HCC827, HCC4006, HCC2935, H1975 (subclone 2), DFCI81, H1650 and drug resistant counterparts were grown in RPMI 1640 (Gibco), 10% FBS and 1% penicillin/streptomycin (Gibco). The PC9 cells were obtained from Dr. Nishio (Kinki University, Osaka, Japan) in 2005. The HCC827 cells were obtained from Dr. Adi Gazdar (UT Southwestern, Dallas, TX) in 2004. The HCC827 EPR cell line was generated by the laboratory of Tetsuya Mitsudomi (Kinki University, Osaka, Japan) in 2011 and the DFCI81 cell line was generated in the Jänne laboratory in 2011. HCC827 + HGF cells were created between 2006 and 2012 by transduction of JP1698-HGF into HCC827 cells, followed by 5 days of 25µg/ml blasticidin selection. PC9 W+T tolerant cell lines were created between 2006 and 2012 by plating 350 cells/well in 96 well format and treating with 100 nM WZ4002 + 30 nM trametinib weekly. Cell line identity was confirmed by fingerprinting (Promega Powerplex 16 System) for the following cell lines: HCC4006, PC9, PC9 PFR3, PC9 GR4, PC9 DR1, PC9 WZR12, PC9 WTR4, HCC827, HCC827 EPR, HCC827 GR6, H1975 subclone 2, HCC2935, HCC2279, and H1650. Fingerprinting was performed in September, 2014 at the Genomic Core Laboratory, Michigan State University. WZ4002 and Torin2 were synthesized using previously published methods (17, 33). Trametinib was synthesized at Haoyuan Chemexpress (Shanghai, China) according to published methods (37). Gefitinib, BMS754807 and crizotinib were purchased from Selleck Chemicals. Stock solutions of all drugs were prepared to 5-10 mM in DMSO and stored at -20°C.

Cell growth and proliferation assays

MTS assays were performed using previously described methods (38). To measure the emergence of acquired resistance, cell lines were plated in triplicate 96 well plates (350 cells/well), with the exception of DFCI81 (700 cells/well). Cells were treated with the indicated drugs the following day and then treatments were exchanged every 7-9 days thereafter. Positive wells were scored as greater than 50% confluent and assessed weekly.

Antibodies and western blotting

Cells were plated at 0.6×10^6 cells per well in 10 cm plates for assessment of ERK1/2 reactivation (Figure 1A). Cells were washed twice with ice cold PBS and lysed in RIPA T-

X100 buffer (Boston Bioproducts). To assess ERK1/2 reactivation (Figure 1B) 0.2×10^6 cells were plated in 6 well plates and treated with the indicated concentration of drugs. Cells were washed once with ice cold PBS and lysed in RIPA T-X100. To assess Bim levels, 0.6×10^6 cells were plated in 10 cm plates, treated with the indicated drugs for 24 hours and lysed with CaspACE 3 lysis buffer (Promega). Immunoblotting was performed according to the antibody manufacturers' recommendations. The following antibodies were purchased from Cell Signaling: anti-phospho-AKT (Ser-473, #4060, 1:2000), total AKT (9272 1:2000), phospho EGFR (Tyr 1068, 3777, 1:1000), total EGFR (2232, 1:1000), phospho ERK1/2 (Thr 202/204, 9101, 1:3000), total ERK1/2 (9102, 1:3000), pS6 (Ser 240/244, 5364, 1:2000), S6 (2217, 1:3000) and BIM (2933, 1:2000). Hsp90 was obtained from Santa Cruz Biotechnology (sc-7947, 1:3000).

Caspase 3 Activity

Cells were plated 0.6×10^6 per 10 cm plate and treated with the indicated drugs the following day. Cells were washed with PBS and resuspended in lysis buffer (CaspACE colorimetric assay, Promega). Non-adherent cells were collected from the media by centrifugation, washed in PBS and added to the lysate. Complete lysis was carried out by rapid freeze thaw cycles. The assay was prepared as suggested by manufacturer protocol using 30 μg of lysate per well and read at 405 nM after an overnight incubation at 37°.

Generation of Mouse Cohorts and Treatment

All care and treatment of experimental animals were in accordance with Harvard Medical School/Dana-Farber Cancer Institute (DFCI) institutional animal care and use committee (IACUC) guidelines. All mice were housed in a pathogen-free environment at DFCI animal facility and handled in strict accordance with Good Animal Practice as defined by the Office of Laboratory Animal Welfare.

WZ4002 was dissolved in 10% NMP (10% 1-methyl-2-pyrrolidinone: 90% PEG-300) and trametinib was dissolved in 0.5% hydroxypropyl methylcellulose with 0.2% Tween™ 80. WZ4002 was dosed as 50 mg/kg daily via PO, trametinib was given as 2.5 mg/kg for five consecutive days followed by three times weekly via PO; the combination dosing schedule and dosage is as same as the single reagents; vehicle control mice were given 10% NMP daily. Torin2 was dissolved in captisol (1:80) followed by dilution in water to 4 mg/ml and was administered at 40 mg/kg daily. Mice treated with Torin2+W+T were initially treated with WZ4002, followed by WZ4002 + trametinib until the development of resistance and then Torin2+W+T.

Doxycycline inducible EGFR L858R-T790M /ccsp-rtTA (TL) transgenic mice were generated as previously described (17, 39). TL mice were fed a doxycycline diet at 6 weeks of age to induce expression of mutant *EGFR*. Mice were evaluated by MRI after 12 to 16 weeks of doxycycline diet to quantify lung tumor burden before being assigned to various treatment study cohorts. All the treatment mice had equal amount initial tumor burden. MRI evaluation was repeated every 2 weeks during the treatment.

Nu/Nu mice were purchase from Charles River Laboratories International Inc. PC9, PC9GR4, and H1975 cell lines were detected as pathogen free in Charles River Laboratories

International Inc. and cultured in RPMI1640 with 10% FBS. The cells were washed with serum-free medium and resuspended in serum-free medium mixed with an equal amount of Matrigel (BD Biosciences). Mice were injected with 2 million cells per shot and 3 spots per mouse. The mice were randomly grouped and treatment was started when the tumors size reached to 100 to 200 mm³. Each cohort included at least 5 mice. Tumor sizes were monitored twice weekly and volumes were calculated with the formula: (mm³) = length × width × width × 0.5.

Histology and immunohistochemistry

Mice were sacrificed with CO₂, half dissected tumors were snap-frozen in liquid nitrogen for preparation of protein lysates or the left was fixed in 10% neutral buffered formalin overnight at room temperature, and then transferred to 70% ethanol, embedded in paraffin, and sectioned at 5 μm for IHC staining. Hematoxylin and eosin (H&E) stains were performed in the Department of Pathology in Brigham and Women's Hospital. Immunohistochemistry for phospho-EGFR, AKT, ERK1/2, S6 and 4EBP1 was using previously described methods (17).

Statistical Analysis

Statistical analysis was performed with GraphPad Prism software. MTS assays are represented as the mean three independent experiments ± SD. *In vivo* experiments are represented as the mean ± SEM. Significance of caspase 3 activity and TUNEL staining was assessed by ordinary one-way ANOVA. Significance of caspase 3 induction was assessed by Fishers exact test. Survival analysis of WZ4002 versus WZ4002 + trametinib treated EGFR LT mice was assessed by the log-rank test.

Supplementary Material

Refer to Web version on PubMed Central for supplementary material.

Acknowledgments

We would like to thank Tetsuya Mitsudomi for providing the HCC827 EPR cell line. We thank Magda Bahcall for helpful discussions and manuscript preparation.

Funding: This study was supported by grants from the National Institutes of Health RO1CA114465 (P.A.J.), RO1CA135257 (P.A.J.), and PO1CA154303 (P.A.J., N.S.G and K.K.W.).

References

1. Mok TS, Wu YL, Thongprasert S, Yang CH, Chu DT, Saijo N, et al. Gefitinib or carboplatin-paclitaxel in pulmonary adenocarcinoma. *N Engl J Med.* 2009; 361:947–57. [PubMed: 19692680]
2. Rosell R, Carcereny E, Gervais R, Vergnenegre A, Massuti B, Felip E, et al. Erlotinib versus standard chemotherapy as first-line treatment for European patients with advanced EGFR mutation-positive non-small-cell lung cancer (EURTAC): a multicentre, open-label, randomised phase 3 trial. *Lancet Oncol.* 2012; 13:239–46. [PubMed: 22285168]
3. Kobayashi S, Boggon TJ, Dayaram T, Janne PA, Kocher O, Meyerson M, et al. EGFR mutation and resistance of non-small-cell lung cancer to gefitinib. *N Engl J Med.* 2005; 352:786–92. [PubMed: 15728811]

4. Pao W, Miller VA, Politi KA, Riely GJ, Somwar R, Zakowski MF, et al. Acquired resistance of lung adenocarcinomas to gefitinib or erlotinib is associated with a second mutation in the EGFR kinase domain. *PLoS Med.* 2005; 2:e73. [PubMed: 15737014]
5. Yu HA, Arcila ME, Rekhtman N, Sima CS, Zakowski MF, Pao W, et al. Analysis of tumor specimens at the time of acquired resistance to EGFR-TKI therapy in 155 patients with EGFR-mutant lung cancers. *Clin Cancer Res.* 2013; 19:2240–7. [PubMed: 23470965]
6. Engelman JA, Zejnullahu K, Mitsudomi T, Song Y, Hyland C, Park JO, et al. MET amplification leads to gefitinib resistance in lung cancer by activating ERBB3 signaling. *Science.* 2007; 316:1039–43. [PubMed: 17463250]
7. Cortot AB, Repellin CE, Shimamura T, Capelletti M, Zejnullahu K, Ercan D, et al. Resistance to irreversible EGF receptor tyrosine kinase inhibitors through a multistep mechanism involving the IGF1R pathway. *Cancer Res.* 2013; 73:834–43. [PubMed: 23172312]
8. Ohashi K, Sequist LV, Arcila ME, Moran T, Chmielecki J, Lin YL, et al. Lung cancers with acquired resistance to EGFR inhibitors occasionally harbor BRAF gene mutations but lack mutations in KRAS, NRAS, or MEK1. *Proc Natl Acad Sci U S A.* 2012; 109:E2127–33. [PubMed: 22773810]
9. Takezawa K, Pirazzoli V, Arcila ME, Nebhan CA, Song X, de Stanchina E, et al. HER2 amplification: a potential mechanism of acquired resistance to EGFR inhibition in EGFR-mutant lung cancers that lack the second-site EGFR T790M mutation. *Cancer Discov.* 2012; 2:922–33. [PubMed: 22956644]
10. Zhang Z, Lee JC, Lin L, Olivas V, Au V, LaFramboise T, et al. Activation of the AXL kinase causes resistance to EGFR-targeted therapy in lung cancer. *Nat Genet.* 2012; 44:852–60. [PubMed: 22751098]
11. Ware KE, Hinz TK, Kleczko E, Singleton KR, Marek LA, Helfrich BA, et al. A mechanism of resistance to gefitinib mediated by cellular reprogramming and the acquisition of an FGF2-FGFR1 autocrine growth loop. *Oncogenesis.* 2013; 2:e39. [PubMed: 23552882]
12. Ware KE, Marshall ME, Heasley LR, Marek L, Hinz TK, Hercule P, et al. Rapidly acquired resistance to EGFR tyrosine kinase inhibitors in NSCLC cell lines through de-repression of FGFR2 and FGFR3 expression. *PLoS One.* 2010; 5:e14117. [PubMed: 21152424]
13. Ercan D, Xu C, Yanagita M, Monast CS, Pratilas CA, Montero J, et al. Reactivation of ERK signaling causes resistance to EGFR kinase inhibitors. *Cancer Discov.* 2012; 2:934–47. [PubMed: 22961667]
14. Sequist LV, Waltman BA, Dias-Santagata D, Digumarthy S, Turke AB, Fidias P, et al. Genotypic and histological evolution of lung cancers acquiring resistance to EGFR inhibitors. *Sci Transl Med.* 2011; 3:75ra26.
15. Sos ML, Koker M, Weir BA, Heynck S, Rabinovsky R, Zander T, et al. PTEN loss contributes to erlotinib resistance in EGFR-mutant lung cancer by activation of Akt and EGFR. *Cancer Res.* 2009; 69:3256–61. [PubMed: 19351834]
16. de Bruin EC, Cowell C, Warne PH, Jiang M, Saunders RE, Melnick MA, et al. Reduced NF1 expression confers resistance to EGFR inhibition in lung cancer. *Cancer Discov.* 2014; 4:606–19. [PubMed: 24535670]
17. Zhou W, Ercan D, Chen L, Yun CH, Li D, Capelletti M, et al. Novel mutant-selective EGFR kinase inhibitors against EGFR T790M. *Nature.* 2009; 462:1070–4. [PubMed: 20033049]
18. Walter AO, Sjin RT, Haringsma HJ, Ohashi K, Sun J, Lee K, et al. Discovery of a mutant-selective covalent inhibitor of EGFR that overcomes T790M-mediated resistance in NSCLC. *Cancer Discov.* 2013; 3:1404–15. [PubMed: 24065731]
19. Cross DA, Ashton SE, Ghiorghiu S, Eberlein C, Nebhan CA, Spitzler PJ, et al. AZD9291, an Irreversible EGFR TKI, Overcomes T790M-Mediated Resistance to EGFR Inhibitors in Lung Cancer. *Cancer Discov.* 2014
20. Janne PA, Ramalingam SS, Yang JC-H, Ahn M-J, Kim D-W, Kim S-W, et al. Clinical activity of the mutant-selective EGFR inhibitor AZD9291 in patients (pts) with EGFR inhibitor-resistant non-small cell lung cancer (NSCLC). *ASCO Meeting Abstracts.* 2014; 32:8009.
21. Sequist LV, Soria J-C, Gadgeel SM, Wakelee HA, Camidge DR, Varga A, et al. First-in human evaluation of CO-1686, an irreversible, highly selective tyrosine kinase inhibitor of mutations of EGFR (activating and T790M). *ASCO Meeting Abstracts.* 2014; 32:8010.

22. Kim D-W, Lee DH, Kang JH, Park K, Han J-Y, Lee J-S, et al. Clinical activity and safety of HM61713, an EGFR-mutant selective inhibitor, in advanced non-small cell lung cancer (NSCLC) patients (pts) with EGFR mutations who had received EGFR tyrosine kinase inhibitors (TKIs). ASCO Meeting Abstracts. 2014; 32:8011.
23. Eberlein CA, Stetson D, Markovets AA, Al-Kadhimi KJ, Lai Z, Fisher PR, et al. Acquired resistance to mutant-selective EGFR inhibitor AZD9291 is associated with increased dependence on RAS signaling in preclinical models. *Cancer Res.* 2015
24. Ogino A, Kitao H, Hirano S, Uchida A, Ishiai M, Kozuki T, et al. Emergence of epidermal growth factor receptor T790M mutation during chronic exposure to gefitinib in a non small cell lung cancer cell line. *Cancer Res.* 2007; 67:7807–14. [PubMed: 17699786]
25. Ercan D, Zejnullahu K, Yonesaka K, Xiao Y, Capelletti M, Rogers A, et al. Amplification of EGFR T790M causes resistance to an irreversible EGFR inhibitor. *Oncogene.* 2010; 29:2346–56. [PubMed: 20118985]
26. Turke AB, Song Y, Costa C, Cook R, Arteaga CL, Asara JM, et al. MEK inhibition leads to PI3K/AKT activation by relieving a negative feedback on ERBB receptors. *Cancer Res.* 2012; 72:3228–37. [PubMed: 22552284]
27. Pratilas CA, Taylor BS, Ye Q, Viale A, Sander C, Solit DB, et al. (V600E)BRAF is associated with disabled feedback inhibition of RAF-MEK signaling and elevated transcriptional output of the pathway. *Proc Natl Acad Sci U S A.* 2009; 106:4519–24. [PubMed: 19251651]
28. Ng KP, Hillmer AM, Chuah CT, Juan WC, Ko TK, Teo AS, et al. A common BIM deletion polymorphism mediates intrinsic resistance and inferior responses to tyrosine kinase inhibitors in cancer. *Nat Med.* 2012; 18:521–8. [PubMed: 22426421]
29. Costa DB, Halmos B, Kumar A, Schumer ST, Huberman MS, Boggon TJ, et al. BIM mediates EGFR tyrosine kinase inhibitor-induced apoptosis in lung cancers with oncogenic EGFR mutations. *PLoS Med.* 2007; 4:1669–79. discussion 80. [PubMed: 17973572]
30. Cragg MS, Kuroda J, Puthalakath H, Huang DC, Strasser A. Gefitinib-induced killing of NSCLC cell lines expressing mutant EGFR requires BIM and can be enhanced by BH3 mimetics. *PLoS Med.* 2007; 4:1681–89. discussion 90. [PubMed: 17973573]
31. Meng J, Fang B, Liao Y, Chresta CM, Smith PD, Roth JA. Apoptosis induction by MEK inhibition in human lung cancer cells is mediated by Bim. *PLoS One.* 2010; 5:e13026. [PubMed: 20885957]
32. Deng J, Shimamura T, Perera S, Carlson NE, Cai D, Shapiro GI, et al. Proapoptotic BH3- only BCL-2 family protein BIM connects death signaling from epidermal growth factor receptor inhibition to the mitochondrion. *Cancer Res.* 2007; 67:11867–75. [PubMed: 18089817]
33. Liu Q, Xu C, Kirubakaran S, Zhang X, Hur W, Liu Y, et al. Characterization of Torin2, an ATP-competitive inhibitor of mTOR, ATM, and ATR. *Cancer Res.* 2013; 73:2574–86. [PubMed: 23436801]
34. Hay N, Sonenberg N. Upstream and downstream of mTOR. *Genes Dev.* 2004; 18:1926–45. [PubMed: 15314020]
35. Corcoran RB, Rothenberg SM, Hata AN, Faber AC, Piris A, Nazarian RM, et al. TORC1 suppression predicts responsiveness to RAF and MEK inhibition in BRAF-mutant melanoma. *Sci Transl Med.* 2013; 5:196ra98.
36. Pirazzoli V, Nebhan C, Song X, Wurtz A, Walther Z, Cai G, et al. Acquired resistance of EGFR-mutant lung adenocarcinomas to afatinib plus cetuximab is associated with activation of mTORC1. *Cell Rep.* 2014; 7:999–1008. [PubMed: 24813888]
37. Gilmartin AG, Bleam MR, Groy A, Moss KG, Minthorn EA, Kulkarni SG, et al. GSK1120212 (JTP-74057) is an inhibitor of MEK activity and activation with favorable pharmacokinetic properties for sustained in vivo pathway inhibition. *Clin Cancer Res.* 2011; 17:989–1000. [PubMed: 21245089]
38. Engelman JA, Mukohara T, Zejnullahu K, Lifshits E, Borrás AM, Gale CM, et al. Allelic dilution obscures detection of a biologically significant resistance mutation in EGFR-amplified lung cancer. *J Clin Invest.* 2006; 116:2695–706. [PubMed: 16906227]
39. Li D, Shimamura T, Ji H, Chen L, Haringsma HJ, McNamara K, et al. Bronchial and peripheral murine lung carcinomas induced by T790M-L858R mutant EGFR respond to HKI-272 and rapamycin combination therapy. *Cancer Cell.* 2007; 12:81–93. [PubMed: 17613438]

Statement of significance

Patients with *EGFR* mutant lung cancer develop acquired resistance to EGFR and mutant selective EGFR tyrosine kinase inhibitors. Here we show that co-targeting EGFR and MEK can prevent the emergence of a broad variety of drug resistance mechanisms *in vitro* and *in vivo* and may be a superior therapeutic regimen for these patients.

Author Manuscript

Author Manuscript

Author Manuscript

Author Manuscript

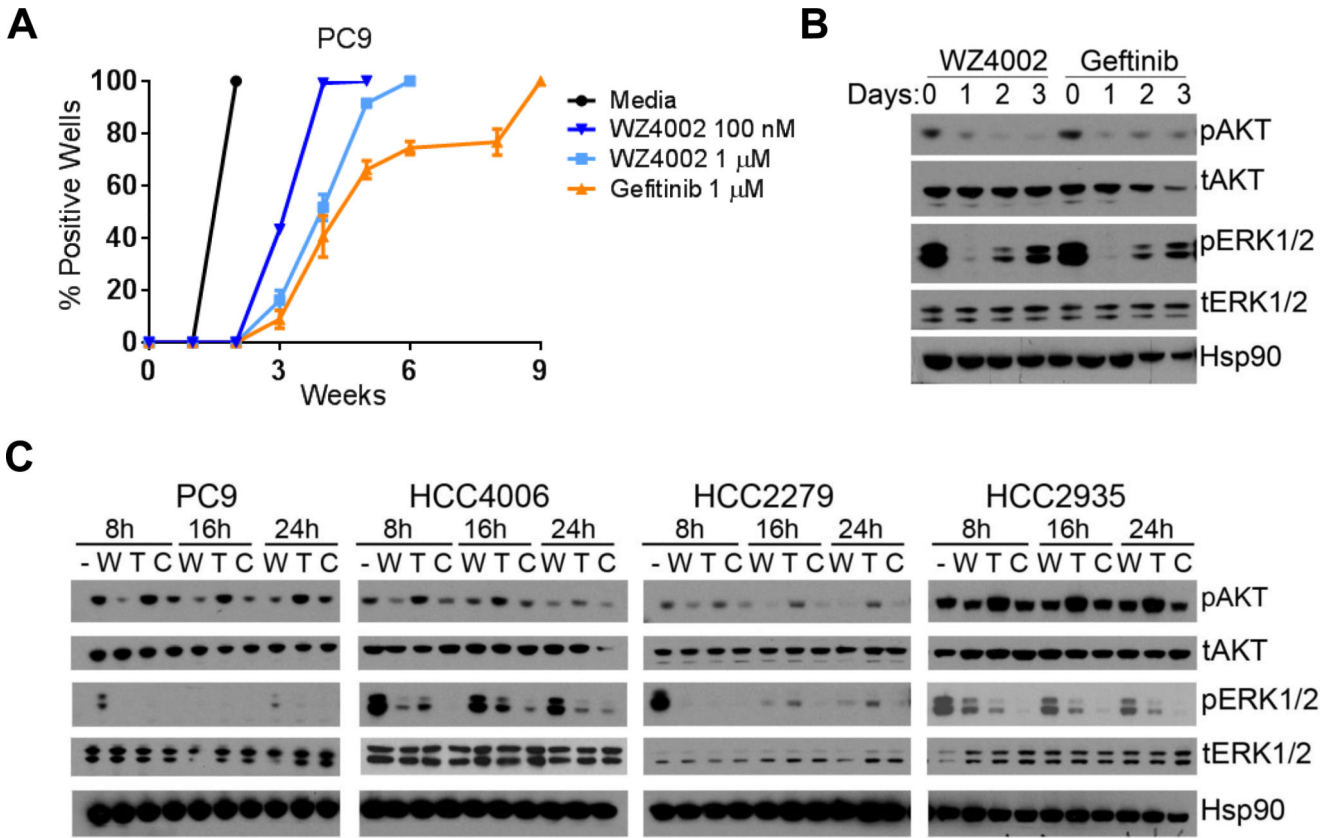


Figure 1. ERK reactivation following EGFR TKI treatment. (A) Cells were treated with DMSO (Media), 100 nM WZ4002, 1 μM of WZ4002 or 1 μM gefitinib weekly (mean +/- SD, n = biological triplicates, 60 wells each). (B) PC9 cells were treated with 1 μM WZ4002 or 1 μM gefitinib and AKT and ERK1/2 phosphorylation was assessed. Hsp90 was assessed as a loading control. Image is representative of three independent experiments. (C) Cell lines were treated with 100 nM WZ4002 (W), 30 nM trametinib (T) or a combination thereof (C) for the indicated time and phosphorylation of AKT and ERK1/2 was assessed by immunoblotting. Image is representative of two independent experiments.

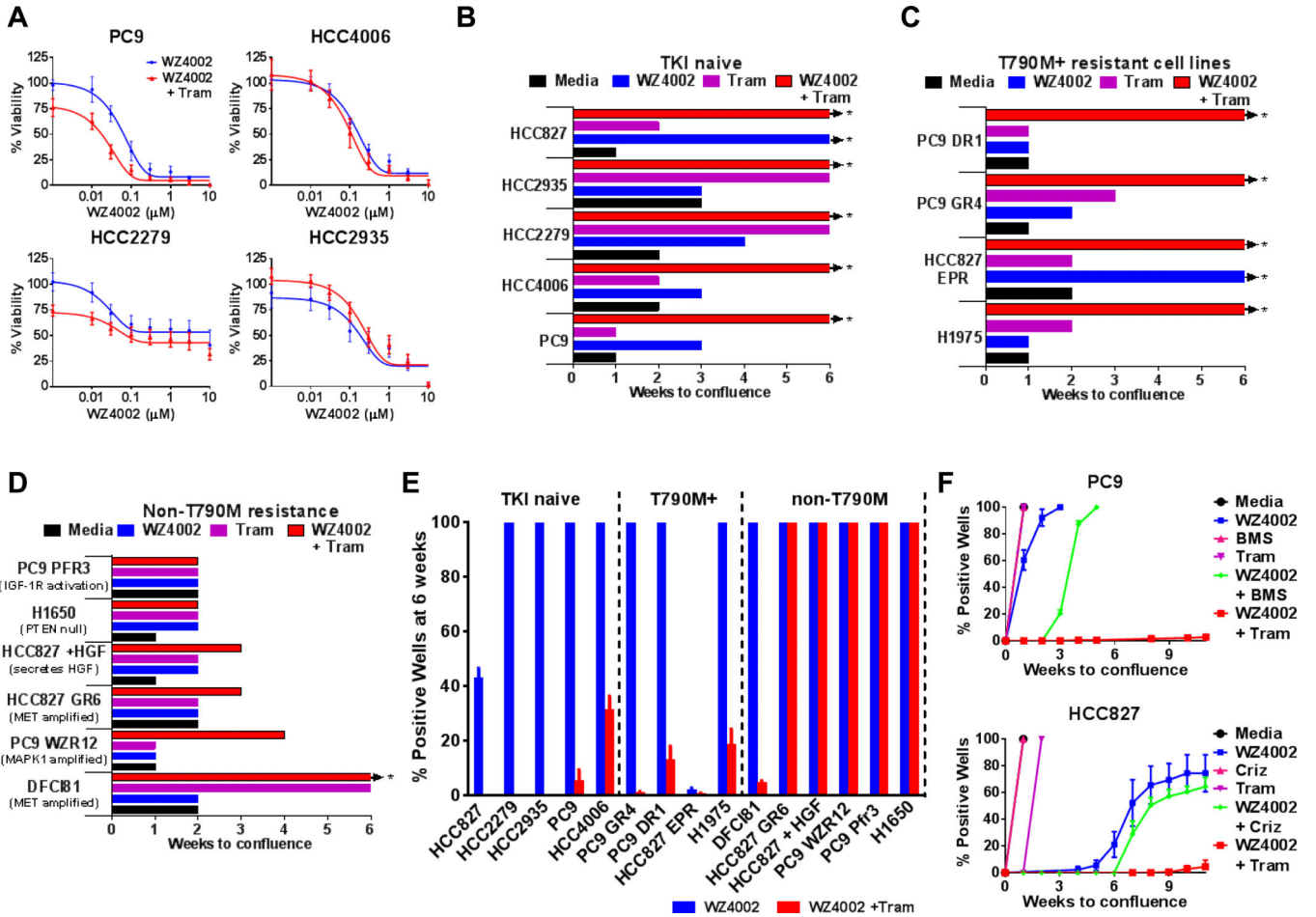
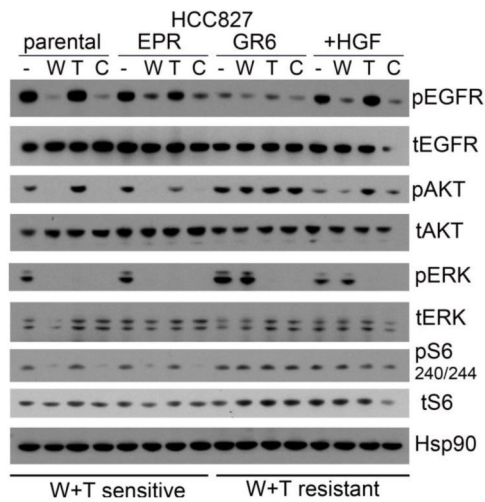
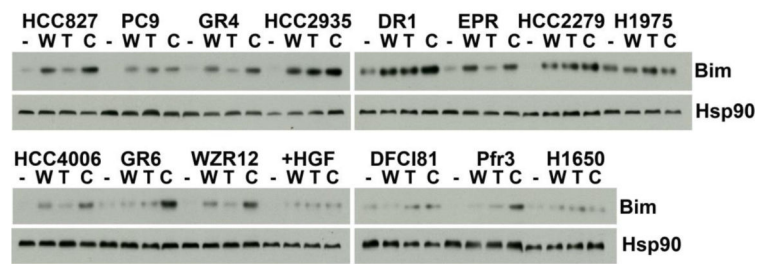


Figure 2. Acquired resistance is prevented by WZ4002 + trametinib combination treatment in TKI naive and T790M+ cell lines. (A) Cell lines were treated with increasing doses of WZ4002 alone or in combination with 30 nM trametinib (Tram) and viability was assessed by MTS (n = 3 independent experiments, mean +/- SD). TKI naive cell lines (B), T790M+ (C) and cell lines harboring non-T790M mechanisms of TKI resistance (D) were treated weekly with 100 nM WZ4002, 30 nM trametinib (Tram) or a combination thereof for 6 weeks. Arrows indicate wells did not achieve 50% confluence by six weeks. Data is representative of 2-3 independent experiments (180 wells per condition). (E) Cell lines were treated with DMSO (Media), 100 nM WZ4002, 30 nM trametinib or a combination thereof and the percentage of wells at 50% or greater confluence were assessed at 6 weeks (n = biological triplicates, 1 plate (60 wells) each). Graph is representative of two or three independent experiments per cell line. (F) PC9 cells were treated with DMSO control (Media), 100 nM WZ4002, 30 nM trametinib (Tram) or 100 nM IGF-1R inhibitor BMS754807 (BMS) or WZ4002 combinations weekly (top panel). HCC827 cells were treated with DMSO (Media), 100 nM WZ4002, 30 nM trametinib, 100 nM crizotinib (Criz) or WZ4002 combinations weekly (bottom panel). Positive wells (n = three biological replicates, 1 plate each) were assessed weekly and graphed mean +/- SD. Each experiment was repeated two times.

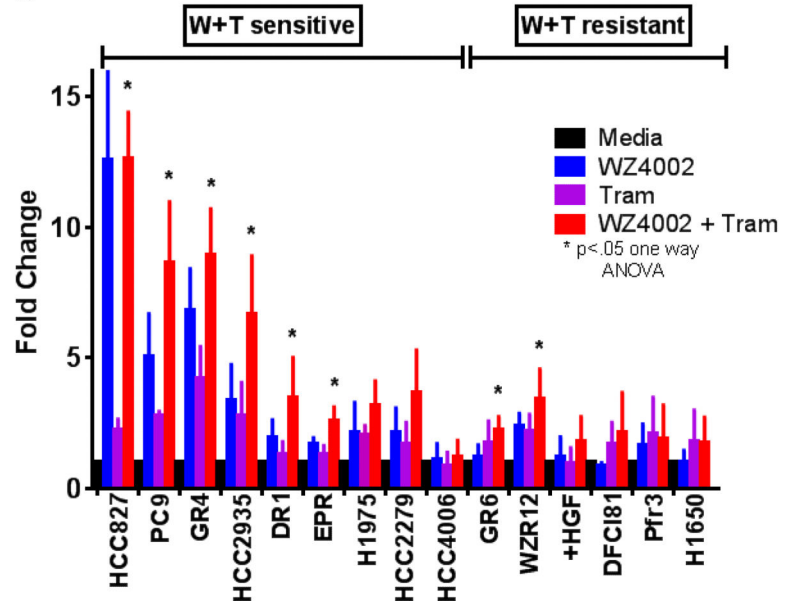
A



B



C

**Figure 3.**

Effect of WZ4002 + trametinib treatment on signaling and apoptosis. (A) Cell lines were treated with DMSO (-), 100 nM WZ4002 (W), 30 nM trametinib (T) or the combination (C) for eight hours and phosphorylation of EGFR, AKT, ERK1/2 and S6 was assessed. Hsp90 was assessed as a loading control. Long term sensitivity or resistance of each cell line to W +T treatment is indicated below the figure. Image is representative of three independent experiments. (B) TKI sensitive and resistant cell lines were treated with 100 nM WZ4002 (W), 30 nM trametinib (T) or a combination thereof (C) for 24 hours and Bim levels were assessed. Hsp90 was used as a loading control. Image is representative of three independent experiments. (C) Cell lines were treated with DMSO control (Media) 100 nM WZ4002, 30 nM trametinib (Tram) or a combination thereof for 72 hours. Caspase 3 activity of lysates was measured and fold change was calculated relative to DMSO control (n = 3 to 4 independent experiments, mean \pm SD). Significance was calculated by one way ANOVA ($p < 0.05$).

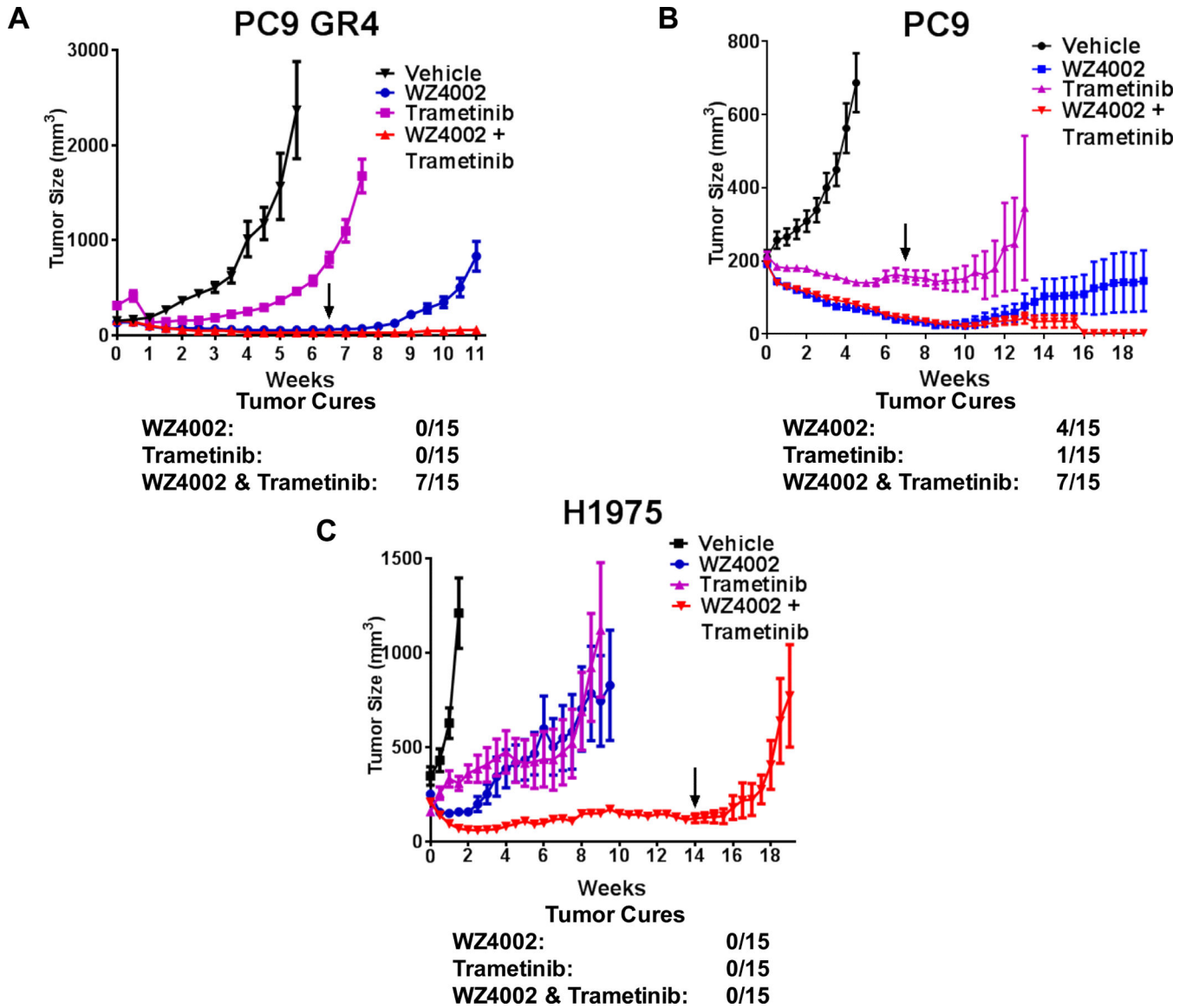


Figure 4. Curative effect of WZ4002 + trametinib treatment *in vivo*. (A) PC9 GR4 xenograft tumors were treated with vehicle control, WZ4002, trametinib (Tram) or the combination thereof (mean \pm SEM, 5 mice per condition). Treatment cessation is indicated by the arrow. Tumor cure is defined as no residual disease beyond treatment cessation. (B) WZ4002 + trametinib treatment is also effective in the TKI naïve PC9 xenograft model (mean \pm SEM, n = 5). (C) WZ4002 + trametinib treatment prevents tumor growth in the H1975 xenograft model but does not result in tumor cures (mean \pm SEM, n = 5).

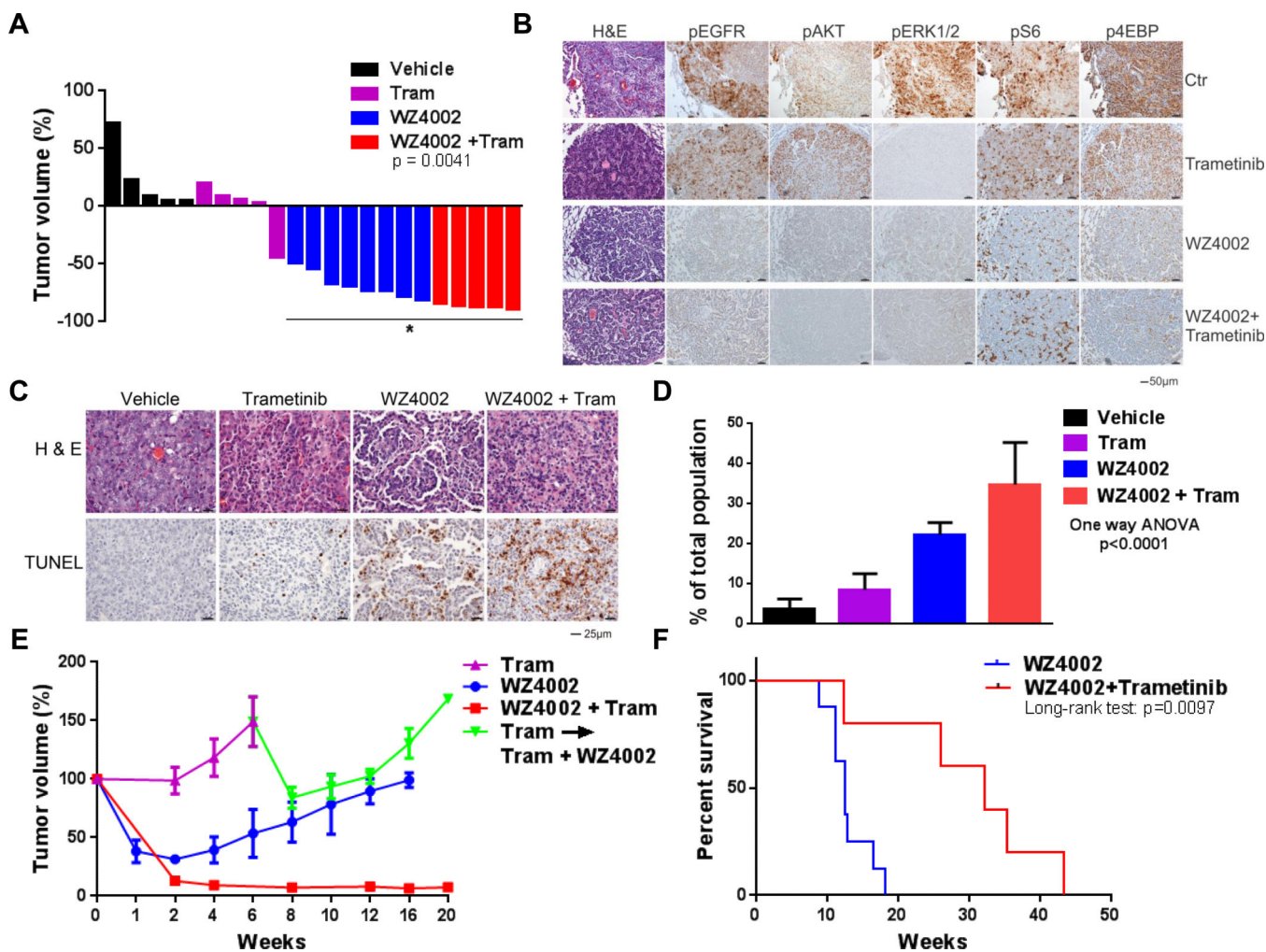
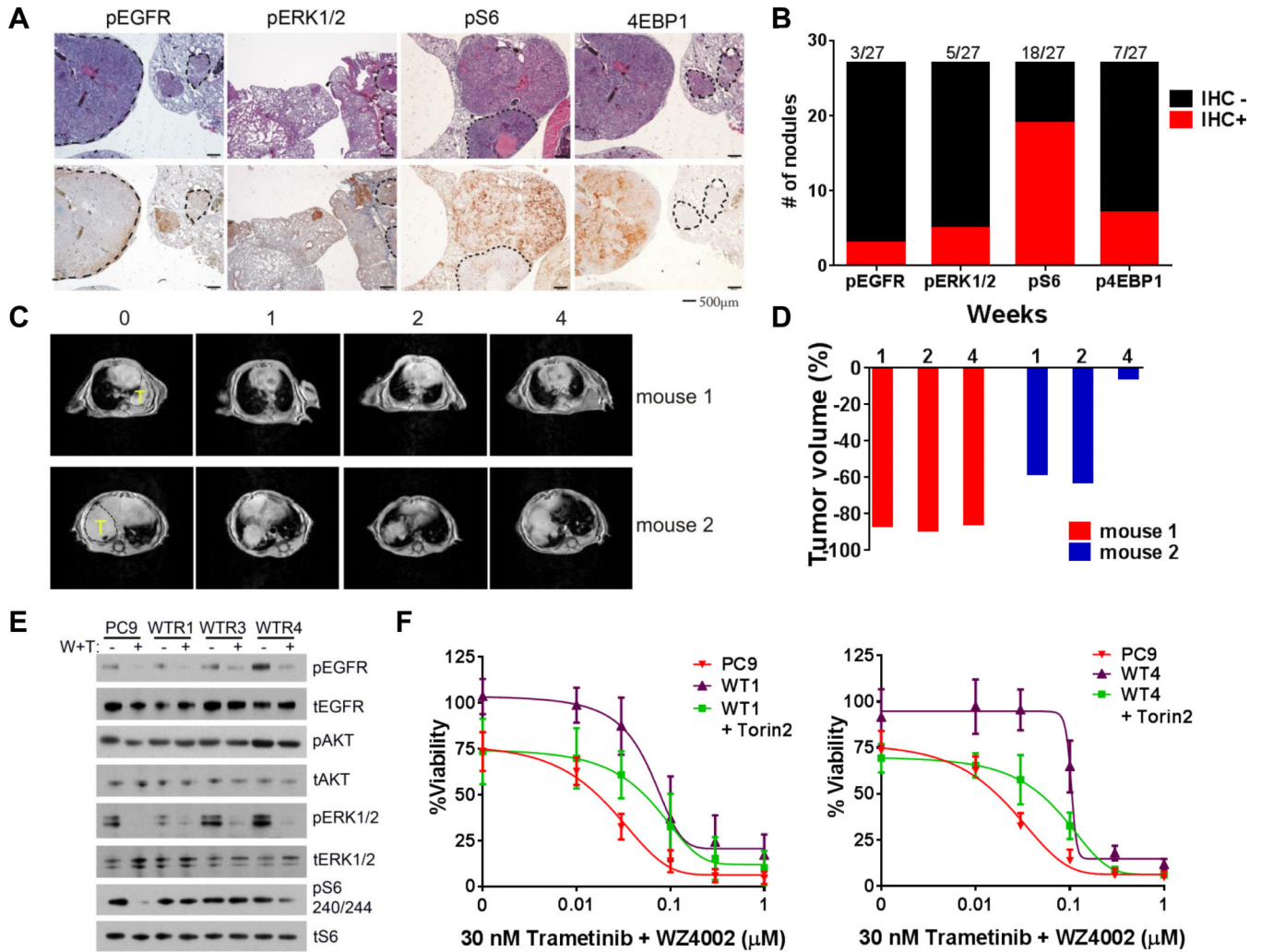


Figure 5. Co-targeting EGFR and MEK prolongs effective treatment duration in *EGFR* L858R/T790M genetically engineered mice. **(A)** Tumor volume after two weeks of vehicle, WZ4002, trametinib or a combination thereof. Significance was assessed by two-tailed t test, $p = 0.0041$. A subset of the WZ4002 alone treated mice are published in a previous report (13). **(B)** Phosphorylation of EGFR, AKT, ERK1/2, S6 and 4EBP1 were assessed by immunohistochemistry after two doses of vehicle, trametinib, WZ4002 or combination. H&E, hematoxylin and eosin. **(C)** Analysis of apoptosis by TUNEL staining after two doses of WZ4002, trametinib or a combination thereof. H&E, hematoxylin and eosin. **(D)** Quantification of TUNEL positive cells. Significance was assessed by one way ANOVA, $p < 0.001$. **(E)** Tumor volume after W+T treatment. Upon tumor growth, mice treated with trametinib (purple line) were treated with a combination of WZ4002 and trametinib (green line). A subset of single agent WZ4002 treated mice was previously reported (13) ($n = 5$, mean \pm SEM). **(F)** Survival of WZ4002 + trametinib treated mice compared to WZ4002 alone. Significance was determined by log-rank test, $p = 0.0097$. One mouse in the combination treatment group was euthanized at 12.3 weeks for a leg problem unrelated to treatment. A necropsy was performed and no tumor was observed (data not shown).

**Figure 6.**

Heterogeneous resistance mechanisms develop in response to WZ4002 + trametinib combination treatment in the *EGFR* L858R/T790M genetically engineered mice. (A) Phosphorylation of EGFR, ERK1/2, S6 and 4EBP1 were assessed by immunohistochemistry and instances of positive nodules aside negative nodules (highlighted with dotted lines) were observed. (B) Total number of tumor nodules IHC positive (red) or negative (black) for EGFR, ERK, S6 and 4EBP1 phosphorylation. Percentage of positive cases is listed above each bar (n = 27). (C) Tumor volume of WZ4002 + trametinib resistant tumors after treatment with a combination of WZ4002, trametinib and Torin2. Yellow T indicates tumor mass. (D) Quantification of tumor volume for each mouse after initiation of WZ4002 + trametinib + Torin2 combination treatment. (E) PC9 derived cell lines tolerant to WZ4002 + trametinib (WT1, 3 and 4) were treated with 100 nM WZ4002 + 30 nM trametinib and phosphorylation of EGFR, AKT, ERK1/2 and S6 were assessed. Image is representative of two independent experiments. (F) Viability of WZ4002 + trametinib tolerant cell lines were assessed after the addition of 10 nM Torin2 to WZ4002 + trametinib co-treatment at 72 hours (n = 3 independent experiments, mean \pm SD).